Research Article

Check for updates

A comparison of sensitivity indices for tolerance design of a transmission mechanism

Zhen-yu LIU[1,3], Han-chao XU[4], Guo-dong SA[2,3✉], Yu-feng LYU[3], Jian-rong TAN[1,3]

[1]*State Key Laboratory of CAD&CG, Zhejiang University, Hangzhou 310027, China*
[2]*Ningbo Research Institute, Zhejiang University, Ningbo 315100, China*
[3]*School of Mechanical Engineering, Zhejiang University, Hangzhou 310027, China*
[4]*Polytechnic Institute, Zhejiang University, Hangzhou 310027, China*

Abstract: Sensitivity analysis is used to quantify the contribution of the uncertainty of input variables to the uncertainty of systematic output responses. For tolerance design in manufacturing and assembly, sensitivity analysis is applied to help designers allocate tolerances optimally. However, different sensitivity indices derived from different sensitivity analysis methods will always lead to conflicting results. It is necessary to find a sensitivity index suitable for tolerance allocation to transmission mechanisms so that the sensitivity results can truly reflect the effects of tolerances on kinematic and dynamic performances. In this paper, a variety of sensitivity indices are investigated and compared based on hybrid simulation. Firstly, the hybrid simulation model of the crank-slider mechanism is established. Secondly, samples of the kinematic and dynamic responses of the mechanism with joint clearances and link length errors are obtained, and the surrogate model established using polynomial chaos expansion (PCE). Then, different sensitivity indices are calculated based on the PCE model and are further used to evaluate the effect of joint clearances and link length errors on the output response. Combined with the tolerance-cost function, the corresponding tolerance allocation schemes are obtained based on different sensitivity analysis results. Finally, the kinematic and dynamic responses of the mechanism adopting different tolerance allocation schemes are simulated, and the sensitivity index corresponding to the optimal response is determined as the most appropriate index.

Key words: Transmission mechanism; Sensitivity analysis; Tolerance allocation; Hybrid simulation; Polynomial chaos expansion (PCE)

1 Introduction

The kinematic and dynamic performances of a transmission mechanism are reflected by its displacement, speed, acceleration, and other data. For example, the vibration performance can be expressed as acceleration fluctuation. These performances of the transmission mechanism are significantly affected by the geometric errors of its parts. The motion stability of the transmission mechanism, such as the crank-slider mechanism, is seriously affected by geometric errors such as joint clearance and link length error. To ensure the comprehensive performance of the mechanism,

✉ Guo-dong SA, sgd@zju.edu.cn

ⓘ Guo-dong SA, https://orcid.org/0000-0001-7803-2270

tolerance design is necessary, which can reasonably control part geometric errors with low cost.

The existing dynamics studies of the mechanism with clearance mainly focus on the construction of contact models for the collision of kinematic pairs (Tian et al., 2018), including the continuous contact model (Haines, 1980), the "separation-contact" two-state model (Dubowsky et al., 1987), the "contact-separation-collision" three-state model (Soong and Thompson, 1990), and the combined model of massless link and spring damping (Seneviratne et al., 1996). These methods can numerically predict kinematic and dynamic performances, considering the clearance and length error. However, there are few studies on tolerance design aiming at optimizing the kinematic and dynamic performances of the transmission mechanism. More in-depth studies are needed.

Tolerance design includes tolerance specification, tolerance modeling, and computer-aided tolerance optimization design (Cai et al., 2004; Cao et al., 2006, 2015). As one of the key steps in the tolerance design process, tolerance allocation has attracted much attention. For example, Lin et al. (2018) proposed a method for motion error analysis of a cycloidal pinion reducer considering manufacturing tolerances, and explored tolerance allocation and optimization using the Monte Carlo method; Dantan et al. (2008) proposed tooth contact analysis, Monte Carlo simulation, and a genetic algorithm for gear tolerance allocation to achieve optimal manufacturing cost; Liu et al. (2019) used the linear regression method to find the mapping relationship between the tolerance zone error of the motion axis and machining accuracy. They carried out a sensitivity analysis to obtain the contribution of the degree of tolerance to the machining accuracy, and finally achieved a reasonable tolerance allocation combined with the tolerance-cost function.

However, state-of-the-art tolerance allocation methods mainly focus on the geometric errors of products rather than their kinematic and dynamic performances, which are very important for the transmission mechanism. Moreover, the above methods are difficult to use to make reasonable performance-oriented tolerance allocation due to the nonlinearity of the kinematic and dynamic models of the transmission mechanism.

Sensitivity analysis provides a feasible way for the performance-oriented tolerance allocation of the transmission mechanism. It is used to quantify the contribution of input variable uncertainty to model output response uncertainty (Saltelli et al., 2008). It can determine the main error affecting the mechanism performance and can provide a theoretical basis for tolerance allocation. For example, Ziegler and Wartzack (2015) proposed a global sensitivity analysis method for convex hull-based tolerance technology to estimate the impact of single part tolerance on assembly clearance in a pin-hole connection. Abbiati et al. (2021) established a sensitivity analysis framework of hybrid simulation by using the Sobol method in the global sensitivity analysis method and obtained the sensitivity of a certain structure response, which reduced the number of experimental samples compared with the Monte Carlo method. Borgonovo et al. (2012) applied the moment independence method in the global sensitivity

analysis method to the field of environmental science to evaluate the impact of input values on the model results. The advantage of the method is that its numerical estimation method reduces the calculation burden. Zhou (2019) used the information entropy method in the global sensitivity analysis method to evaluate the effect of each parameter on bolt stress. The advantage is that the output variable is allowed to be a multidimensional variable.

In the above studies, the sensitivity analysis has shown its value well, but the following problems remain:

(1) The above sensitivity analysis methods can be applied to a transmission mechanism; however, the results are not consistent in most cases. This is because these methods are different in principle, which leads to their different objects of application. For example, Borgonovo (2007) proposed a moment-independent method that can be defined in the presence of correlations among the inputs, whereas the Sobol method requires independent inputs. Therefore, it is necessary to find a sensitivity analysis method, suitable for the performance-oriented tolerance allocation of the transmission mechanism, which can truly reflect the effect of geometric errors on performance.

(2) For many complex nonlinear physical systems, the sensitivity index cannot be analytically solved and can only be estimated by a numerical method based on a sample. However, the sample size of physical experiments is always limited due to their high cost and to the inability to modify the size of parts, while the data obtained by simulation is time-consuming with low accuracy. Therefore, it is necessary to build a high-accuracy simulation model to obtain samples and then to calculate the sensitivity index quickly through surrogate model technology.

In this study, we proposed a comparison method of the sensitivity indices based on hybrid simulation, so as to determine the optimal sensitivity index that accurately reflects the impact of geometric errors on the kinematic and dynamic performances of the transmission mechanism as shown in Fig. 1. Firstly, we established a hybrid simulation model including a real experiment platform and a simulation model, where the parameters of the simulation model were calibrated according to the experimental data. Secondly, the combined sample of clearance and link length was generated by a classic sampling method, Latin hypercube sampling (LHS), which can effectively improve the
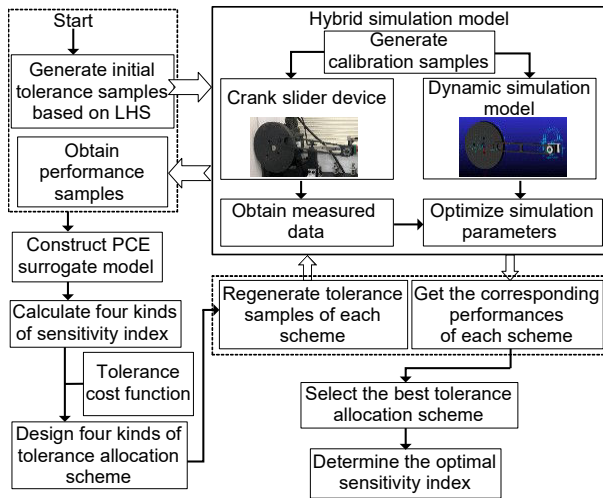
Fig. 1 Approach framework for comparing sensitivity indices based on the hybrid simulation model

uniformity of sample points in design space. The corresponding kinematic and dynamic performances of the mechanism were calculated based on the hybrid simulation model performance. Then, the polynomial chaos expansion (PCE) method, a method that can effectively deal with system uncertainty caused by input random variables, was used to construct the surrogate model, and the sensitivity of the kinematic and dynamic performances of the machine to the joint clearance and link length errors was calculated based on the surrogate model. Finally, the tolerance was allocated according to the results of each sensitivity analysis method combined with the cost-tolerance function, and the sensitivity analysis method was determined by comparison.

This paper is organized as follows: Section 2 introduces four popular sensitivity indices; Section 3 shows the proposed hybrid simulation model in detail; Section 4 proposes the comparison method of sensitivity indices and gives detailed experimental results; Section 5 discusses the limitations of our study and how future work could be carried out; Section 6 summarizes the whole paper.

2 Introduction of sensitivity indices

The purpose of sensitivity analysis is to explore the distribution of model output uncertainty with respect to input uncertainty (Saltelli and Tarantola, 2002). Considering that the experimental purpose is

to research the sensitivity of the kinematic and dynamic performances of the crank-slider mechanism to errors of clearance and link length, this paper selects four of the popular sensitivity analysis methods for research and comparison, as follows: linear regression method, variance-based method, moment-independent method, and information-entropy method.

2.1 Linear regression method

Linear regression (Darlington and Hayes, 2016) is a statistical analysis method that uses regression analysis in mathematical statistics to determine the quantitative relationship between two or more variables. Linear regression is a powerful tool determining relations among system output y and input variables X. It focuses on the first-order effects (the main effects) of X on y, and ignores the higher-order effects (the nonlinear effects). In most cases, the higher-order effects are much smaller than the first-order effects. Therefore, linear regression can be used not only for sensitivity analysis of linear models, but also for nonlinear models.

For a linear model, we assume that its expression is

$$y = a_0 + \sum_{i=1}^{k} a_i x_i, \qquad (1)$$

where y is the response value of the model, a_0 is the initial value, $X = \{x_1, x_2, \cdots, x_k\}$ is the set of input variables, and a_i is the coefficient of each input variable.

The linear regression method first needs to experiment with the model. Randomly sampling the input variables gives a matrix M with a sample space of N rows and k columns. The response y of each row of the matrix M is obtained experimentally and by getting an N-row output vector Y, where N is the scale of the experiment and the number of rows of the matrix M. In theory, the larger the size of N, the more accurate the prediction model. After obtaining much experimental data, we can carry out simple linear regression to obtain the expression of the prediction model:

$$y = b_0 + \sum_{i=1}^{k} b_i x_i, \qquad (2)$$

where b_0 and b_i are calculated by the least square method according to the square difference between

the linear regression y and the experimental y. It should be noted that due to errors in the experimental data, the prediction model is often different from the actual model, which is also the reason for using b_0 and b_i. To reduce this error, we can increase the size of N or optimize the loss function.

The sensitivity of y to x_i is

$$\beta_{x_i} = \frac{b_i}{\sum_{i=1}^{k} b_i}. \tag{3}$$

2.2 Variance-based method

The Sobol method is a widely used sensitivity analysis method (Sobol, 1993). It uses variance to describe the uncertainty between input variables and the output response of the model and considers the interactions between input variables.

For a model, we assume that its expression is

$$Y = g(X). \tag{4}$$

Assume that the spatial domain of X is Ω_X. The input variables are independent of each other and follow a joint probability density function (PDF):

$$f_X(X) = \prod_i^k f_{x_i}(x_i), \tag{5}$$

where f_{x_i} is the PDF of x_i.

The Sobol method holds that for any square-integrable function $g(X)$, the function can be decomposed into the sum of its sub-terms:

$$Y = g_0 + \sum_{i=1}^{k} g_i(x_i) + \sum_{1 \leq i \leq j \leq k} g_{ij}(x_i, x_j) + \cdots + g_{12\cdots k}(X), \tag{6}$$

where g_0 is the expectation of Y, and g_i, g_{ij}, and $g_{12\cdots k}$ are the coefficients for each item. Eq. (6) can also be written as

$$Y = g_0 + \sum_{u \neq \varnothing} g_u(X_u), \tag{7}$$

where $u = \{i_1, i_2, \cdots, i_s\} \subset \{1, 2, \cdots, k\}$ are index sets, g_u is the coefficient of each item, and X_u is a sub-vector

of X. In the above equation, the number of summation terms is $2^k - 1$.

The Sobol decomposition is unique under the condition:

$$\int_{\Omega_x} g_u(X_u) f_{x_m}(x_m) \, dx_m = 0, \quad m \in u. \tag{8}$$

This condition means that the mean of each term is 0, which means that all the terms in the expansion are orthogonal to each other. Uniqueness and orthogonality allow the variance D of Y to be decomposed as follows:

$$D = \mathrm{Var}[g(X)] = \sum_{u \neq \varnothing} D_u, \tag{9}$$

where D_u denotes the partial variance:

$$D_u = \mathrm{Var}[g_u(X_u)] = E[g_u^2(X_u)]. \tag{10}$$

Since the mean of each term in the expansion is 0, the variance of each term is the expectation of each term squared. The Sobol index S_u is

$$S_u = \frac{D_u}{D}, \tag{11}$$

where $\sum_{u \neq \varnothing} S_u = 1$.

The first-order index $S_i^{(1)}$ describes the effect of an input variable x_i. The second-order index $S_{ij}^{(2)}$ describes the interactions of $\{x_i, x_j\}$. The higher-order sensitivity quantifies the interactions of more input variables. The total sensitivity index $S_i^{(\mathrm{tot})}$ represents the total effect of an input variable x_i and explains the interaction between its main effect and all other input variables. Its expression is

$$S_i^{(\mathrm{tot})} = 1 - S_{\sim i}, \tag{12}$$

where $S_{\sim i}$ is the sum of all S_u with u not including i.

There are mainly three methods to calculate Sobol indices: Monte Carlo simulation method (Sobol, 2001), Fourier amplitude sensitivity test (Cukier et al., 1973), and proxy model method (Sudret, 2008). The proxy model constructed by PCE can directly obtain Sobol indices and requires fewer samples than the Monte Carlo simulation method.

2.3 Moment-independent method

The moment-independent method (Borgonovo, 2007) is a sensitivity analysis method based on probability distribution, which can reflect the effects of random variables on the entire probability distribution function of the output response. It can reflect the uncertainty of random variables more comprehensively.

Assuming that X is a set of k independent input variables when each input variable obeys a certain distribution, its uncertainty will be passed to the output response Y through $g(X)$, so that Y also obeys a certain distribution.

The PDF and cumulative distribution function (CDF) of Y are $f_Y(y)$ and $F_Y(y)$. When x_i is a definite value $x_i^{(j)}$, the conditional PDF and the conditional CDF of Y can be expressed as $f_{Y|x_i=x_i^{(j)}}(y)$ and $F_{Y|x_i=x_i^{(j)}}(y)$. Fig. 2 shows the curves of the above functions.
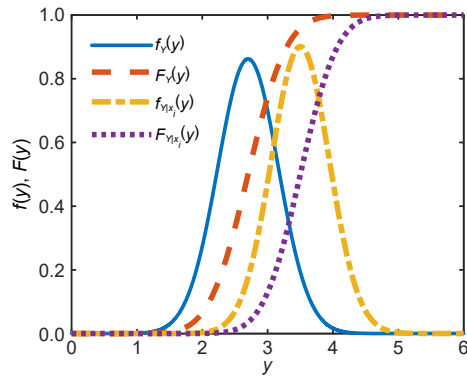

Fig. 2 Unconditional and conditional CDF and PDF for Y

When x_i is $x_i^{(j)}$, the area difference of $f_y(y)$ can be expressed as

$$\alpha(x_i) = \int \left| f_Y(y) - f_{Y|x_i=x_i^{(j)}}(y) \right| \mathrm{d}y. \tag{13}$$

When $x_i^{(j)}$ changes in the entire distribution range, the mean of the above area difference can be expressed as

$$E_{x_i}\left[\alpha(x_i) \right] = \int \alpha(x_i) f_{x_i}(x_i) \, \mathrm{d}x_i. \tag{14}$$

The moment-independent sensitivity index based on a PDF is

$$S_i^{(\mathrm{PDF})} = \frac{E_{x_i}\left[\alpha(x_i) \right]}{2}, \tag{15}$$

where $E_{x_i}\left[\alpha(x_i) \right]$ divided by two is for normalization.

2.4 Information-entropy method

Information-entropy (Shannon, 1948) is a concept in information theory describing the degree of uncertainty of information sources, and is deduced from the definition of entropy in thermodynamics. It can represent the disorder degree of the system. The greater the entropy is, the more chaotic the system is, which makes prediction more difficult. When the entropy is zero, the system eliminates the effects of uncertain factors, and the output is a deterministic result. The information-entropy method is a new global sensitivity analysis method, which uses the change of entropy to predict the importance of input variables to output response.

The output response Y of the model is divided into one and multi-dimensional vectors, and there are two types: continuous and discrete. When Y is a 1D continuous variable, its spatial domain is Ω_Y, its PDF is $f_Y(y)$, and the information entropy of Y can be expressed as

$$H(Y) = -\int_{\Omega_Y} f_Y(y) \log_r f_Y(y) \, \mathrm{d}y, \tag{16}$$

where r is the base of the logarithm function, generally not less than 2.

X is the set of input variables corresponding to Y. When a certain input variable is fixed, such as $x_i = x_i^{(j)}$, the PDF of Y changes from $f_Y(y)$ to the conditional PDF $f_{Y|x_i=x_i^{(j)}}(y)$, and the conditional information entropy of Y at $x_i^{(j)}$ can be obtained, which can be expressed as

$$H\left(Y \middle| x_i = x_i^{(j)}\right) = -\int_{\Omega_Y} f_{Y|x_i=x_i^{(j)}}(Y) \log_r f_{Y|x_i=x_i^{(j)}}(Y) \, \mathrm{d}Y. \tag{17}$$

To calculate $H(Y) - H\left(Y \middle| x_i = x_i^{(j)}\right)$ of x_i overall range, their mean is the effect of x_i on the overall uncertainty of output response Y. Multiple values $\{x_i^{(1)}, x_i^{(2)}, \cdots, x_i^{(l)}\}$ in the value range of x_i are sampled to calculate the global sensitivity index S_{x_i}, which is expressed as

$$S_{x_i} = \frac{\sum_{k=1}^{l}\left[H(Y) - H\left(Y \mid x_i = x_i^{(k)}\right)\right]}{l}. \qquad (18)$$

The larger S_{x_i} is, the greater the change of information entropy of Y will be after the uncertainty of x_i is eliminated, which indicates that the sensitivity of Y to X is higher.

3 Hybrid simulation model enhanced by measured data

In this section, we propose a hybrid simulation model of a crank-slider mechanism. Limited physical experiment data was used to support the verification and calibration of the simulation model, which could guarantee its accuracy.

3.1 Crank-slider experiment platform

The crank-slider experiment platform is composed of an actuator, a motor drive device, and a data acquisition (DAQ) system. The actuator includes a crank disc, connecting rod, slider, connecting shaft, and other supporting parts. A rigid connection is adopted between the experimental platform and the experimental table. The experimental platform is shown in Fig. 3, and the schematic plot of the experimental platform is shown in Fig. 4.
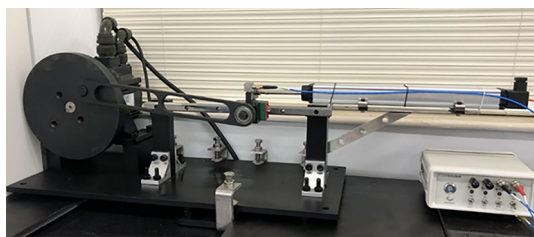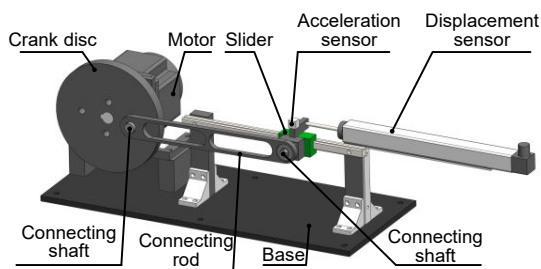

Fig. 3 Crank-slider experiment platform

Fig. 4 Schematic plot of the experimental platform

The DAQ system includes a pull rod displacement sensor and a triaxial acceleration sensor. The displacement sensor sends the displacement information of the slider to the DAQ card by voltage, and then the data is transmitted to the computer at a certain sampling frequency by the DAQ card. The voltage signal of the acceleration sensor is small and easily interfered with, so a constant current adapter is installed between it and the DAQ card to filter and amplify the signal. Displacement data and acceleration data can be converted into velocity data by differential and integral processing respectively, and they can be cross-verified to improve the reliability of experimental data. Each device is shown in Fig. 5.
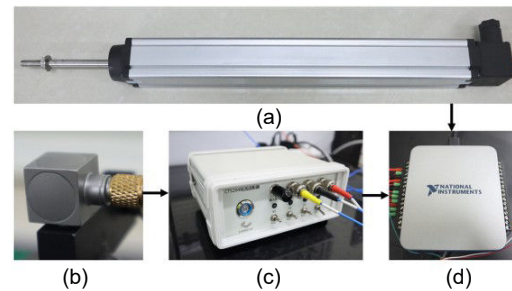

Fig. 5 DAQ system: (a) displacement sensor; (b) acceleration sensor; (c) constant current adapter; (d) DAQ card

The crank-slider mechanism has a fixed crank length, connecting rod length, and aperture size at both ends of the connecting rod. By changing the connecting shaft with different diameters, impact dynamics experiments under different gaps were carried out, and the kinematic and dynamic performances of the mechanism were obtained. The clearance between the connecting shaft and the connecting rod is shown in Fig. 6, and the dimension parameters are shown in Fig. 7.

In Fig. 7, half the difference between the left aperture of the connecting rod H_L and the left connecting shaft diameter S_L is the radius clearance ΔR_L, and half the difference between the right aperture of the connecting rod H_R and the right connecting shaft diameter S_R is the radius clearance ΔR_R. That is because, when there is clearance at both ends of the connecting rod, the connecting rod lacks axial fixing, so only one end of the test is allowed to have clearance, and the other end is axially fixed by a rolling bearing, where the clearance is approximately zero. The three connection modes in the experiments are shown in Fig. 8.
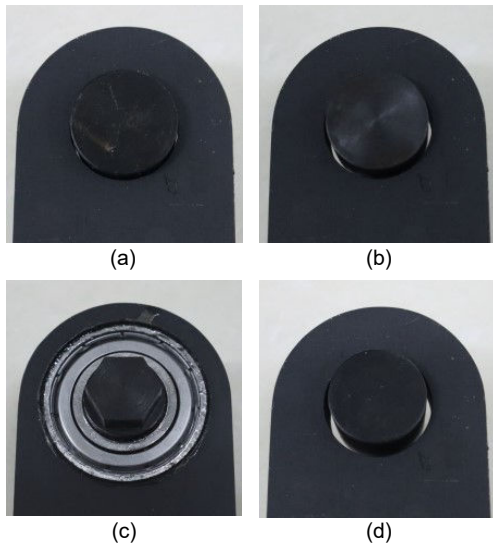
Fig. 6 Radius clearance (ΔR) between the connecting shaft and connecting rod: (a) ΔR=0.0 mm; (b) ΔR=0.2 mm; (c) ΔR=0.6 mm; (d) ΔR=1.0 mm
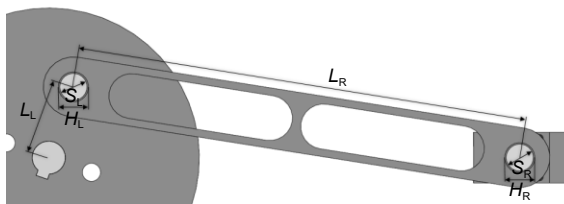

Fig. 7 Dimension parameters of the crank-slider mechanism parts (L_L is the length of the crank, and L_R the length of the connecting rod)
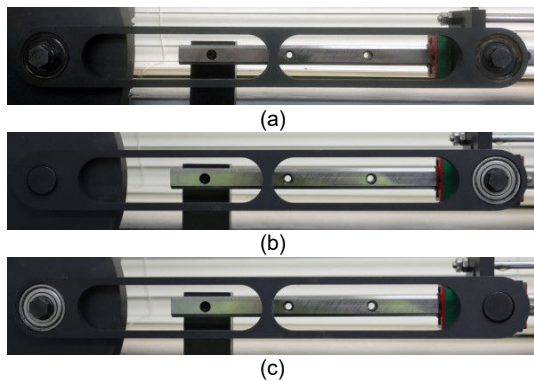

Fig. 8 Three connection modes in the experiments: (a) no joint clearance at both ends; (b) joint clearance on the left; (c) joint clearance on the right

Through different combinations, the experimental data of the crank-slider mechanism with different joint clearances at various speeds can be obtained by this experimental platform, which contains 40 samples. Some specific parameters are shown in Table 1.

Table 1 Experimental parameters

Trial	ΔR_L (mm)	ΔR_R (mm)	Speed (r/min)
1	0.2	0.0	180
2	0.4	0.0	180
3	0.6	0.0	180
4	0.8	0.0	180
5	1.0	0.0	180
6	0.2	0.0	240
⋮	⋮	⋮	⋮
14	0.8	0.0	300
15	1.0	0.0	300
⋮	⋮	⋮	⋮
39	0.0	0.8	360
40	0.0	1.0	360

Experimental data corresponding to each parameter and reflecting the kinematic and dynamic performances of the mechanism were obtained. Partial experimental results are shown in Figs. 9 and 10.
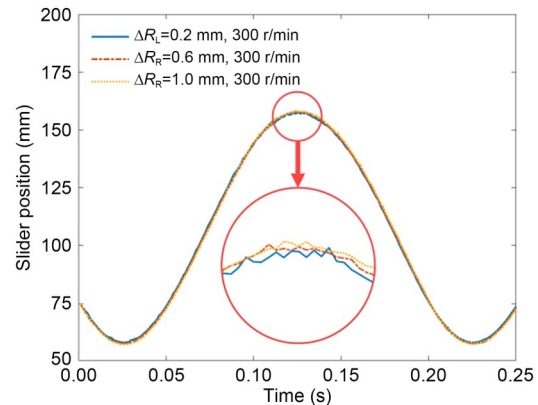

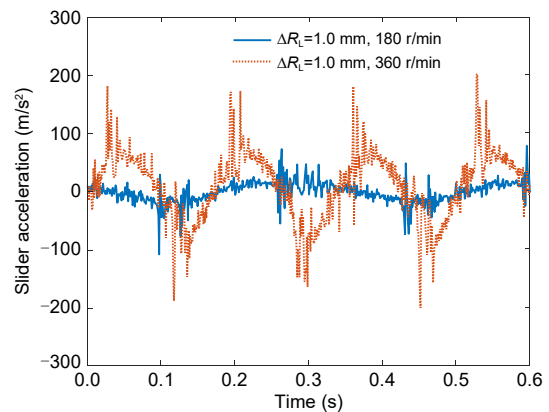**Fig. 9 Experimental slider displacement data**

Fig. 10 Experimental slider acceleration data

Based on all the experimental data, several facts were observed:

(1) With the increase of the joint clearance, the deviation of the slider displacement curve near the motion pole of the mechanism increases.

(2) The acceleration curve of the slider shows significant oscillation near the pole position of the mechanism, and the larger the joint clearance is, the larger the oscillation amplitude is.

(3) Under the same joint clearance, the higher the motor speed, the greater the oscillation amplitude of the slider acceleration curve near the pole position of the mechanism.

(4) Compared to the acceleration of the slider, the joint clearance has little effect on the displacement of the slider.

Therefore, the joint clearance indeed seriously affects the dynamic performance, and the variance of the slider acceleration data is considered as the output response to reflect the kinematic and dynamic performances of the mechanism.

3.2 Simulation model enhanced by physical experiment

To establish the simulation model of the crank-slider mechanism and obtain the acceleration data of the slider, we used MSC ADAMS to simulate the mechanism. The functions of MSC ADAMS are focused on the modeling, analysis, and optimization of multi-body mechanical systems (Ambaye and Lemu, 2021), which can be used to predict the performances of mechanical systems, motion range, and collision detection. The simulation model of the no-clearance crank-slider mechanism is shown in Fig. 11.
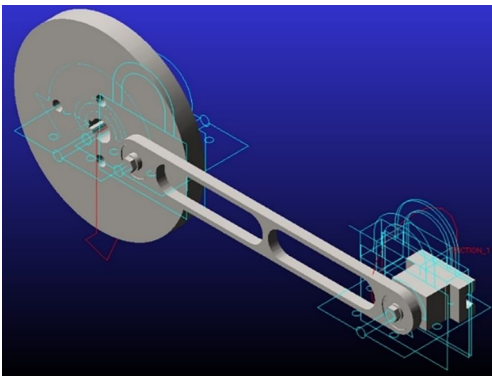

Fig. 11 Simulation model of the ideal crank-slider mechanism

The geometric and material parameters of the simulation model are the same as those of the real model.

To extract the variance reflecting the fluctuation degree of the slider acceleration, it is necessary to first obtain the slider acceleration data under the ideal no-clearance condition. Simulation and experimental data for the no-clearance acceleration at four different speeds are shown in Fig. 12.

Secondly, the acceleration performance of the slider is mainly related to the impact at the joint clearance. To make the simulation model reflect the collision situation of the physical model, it is very important to set the contact parameters reasonably. In MSC ADAMS, the parameters affecting contact collision include stiffness, force exponent, damping, and penetration depth. We used the method of comparison with the experimental platform data, took the acceleration as the measurement index, constantly adjusted these four parameters, and finally got a reasonable parameter. By changing the clearance and speed of the simulation model, the same experiment as the experimental platform was carried out, and 40 sets of simulation data were obtained. The simulation results were compared with the experimental platform data, and part of the comparison is shown in Fig. 13.

According to Fig. 13, the simulation data are in good agreement with the physical experiment data. To quantify the accuracy of the simulation data, the variance of the difference between the simulation acceleration data and the ideal no-clearance acceleration data and the variance of the difference between the experimental acceleration data and the ideal no-clearance acceleration data were calculated. The magnitude of the variance reflects the fluctuation degree of the slider acceleration. Some calculated values are shown in Table 2.

The calculated results were classified according to the speed, and the average errors between simulation variance and experimental variance at 180, 240, 300, and 360 r/min are 9.86%, 11.86%, 7.98%, and 9.55%, respectively. Analysis shows that at all four different speeds, the best speed for the simulation model to simulate the kinematic and dynamic performances of the crank-slider mechanism is 300 r/min.

3.3 Random sampling of input variables

For the hybrid simulation model of the crank-slider mechanism, its input variables include ΔR_{L}, ΔR_{R}, the length of the crank L_{L}, and the length of the connecting rod L_{R} (Fig. 7). According to the central limit theorem, when the number of samples is large, the
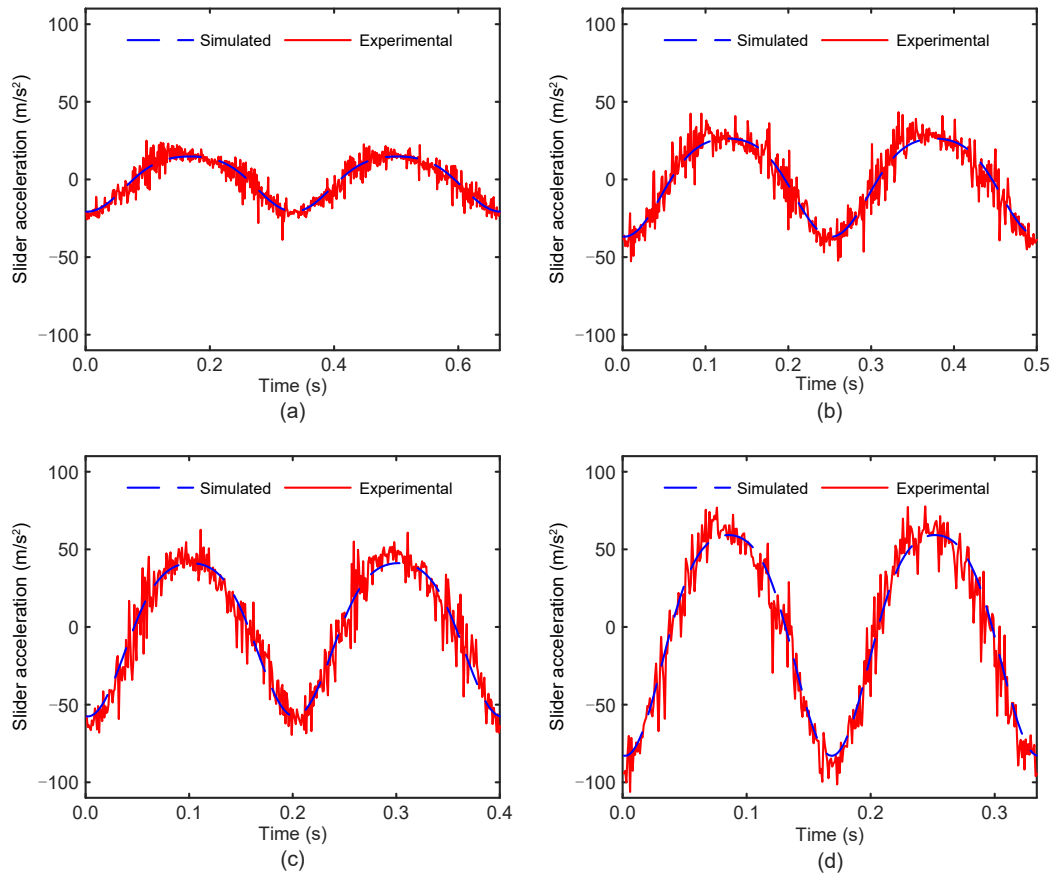
Fig. 12 Simulated and experimental slider acceleration data under the no-clearance condition at four different speeds: (a) 180 r/min; (b) 240 r/min; (c) 300 r/min; (d) 360 r/min

sum of multiple random variables obeying arbitrary distribution tends to a normal distribution. Therefore, random variables in engineering are often assumed to obey normal distribution. We assume that each input variable is a random number that obeys a normal distribution in each tolerance zone or limit clearance.

The range of tolerance zone and limit clearance increases with the reduction of tolerance class. To maximize the scope of the experiment and provide more comprehensive experimental data, we selected the tolerance grade of IT12. The value range and normal distribution of each input variable are shown in Table 3.

The normal distribution of each input variable was determined and random sampling was carried out. The PCE surrogate model requires fewer sample data and, among the existing sampling methods, LHS (McKay et al., 2000) has the advantages of both Monte Carlo random sampling and stratified sampling. The LHS method ensures the uniformity of a small number of samples and is one of the best small sample

simulation methods (Helton and Davis, 2003). Therefore, the LHS method was used to sample input variables and obtain 100 groups of sample data, some of which are shown in Table 4.

3.4 Experiment based on the hybrid simulation model

The hybrid simulation model is a simulation model obtained through the verification and calibration of physical experimental data, as shown in Fig. 14.

The simulation effect of this model was better at 300 r/min, so the experiment was carried out at this speed. One hundred sets of sample data were input to obtain the slider acceleration data of five cycles in the process of uniform rotation of the corresponding hybrid simulation model. After subtracting them from the acceleration data of the slider of the ideal no-clearance mechanism at the same speed, the variance of the difference value was obtained to reflect the kinematic and dynamic performances of the mechanism. The
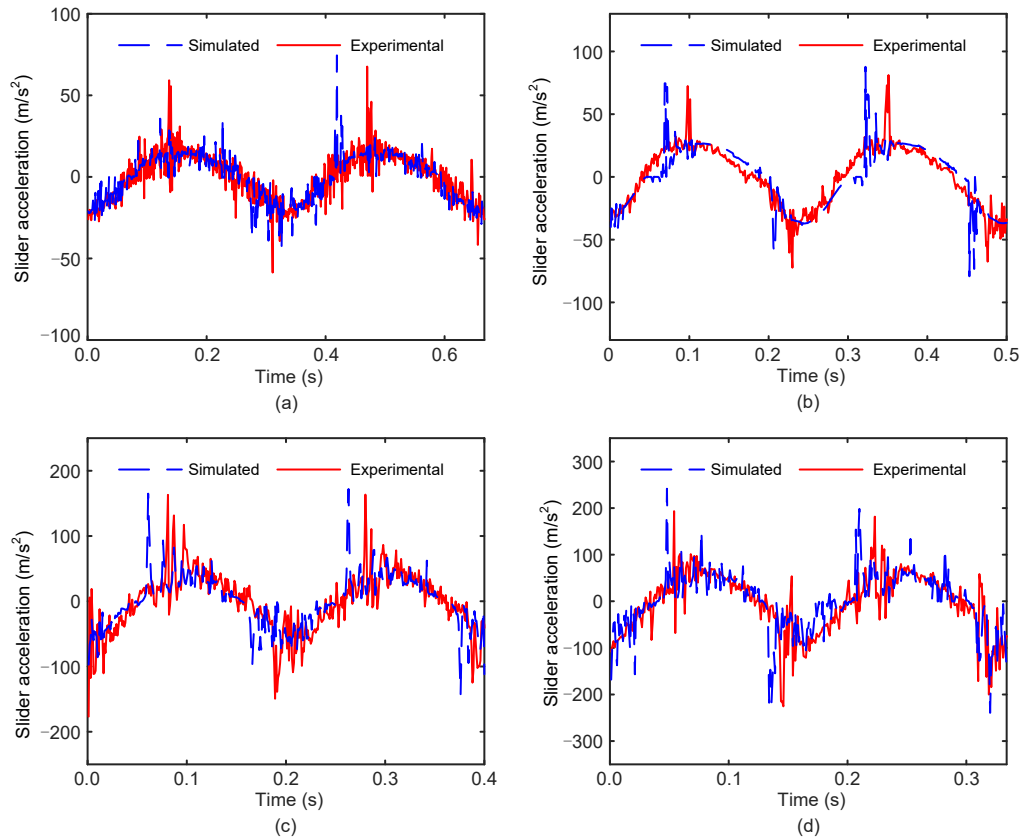
Fig. 13 Comparison of simulation and experimental data on slider acceleration: (a) ΔR_L=0.2 mm, 180 r/min; (b) ΔR_R=1.0 mm, 240 r/min; (c) ΔR_L=0.8 mm, 300 r/min; (d) ΔR_L=0.4 mm, 360 r/min

Table 2 Comparison among simulation, experiment, and ideal data

Speed (r/min)	ΔR_L (mm)	ΔR_R (mm)	Variance of simulation	Variance of experiment	Error (%)
180	0.2	0.0	13.77	15.22	9.53
240	0.0	1.0	35.45	40.11	11.62
300	0.8	0.0	204.81	223.66	8.43
360	0.4	0.0	432.87	398.06	8.74

Table 3 Value range and normal distribution of each input variable

Item	ΔR_L (mm)	ΔR_R (mm)	L_L (mm)	L_R (mm)
Value range	[0, 0.21]	[0, 0.21]	[49.875, 50.125]	[299.74, 300.26]
Normal distribution	N(0.105, 1.15×10⁻³)	N(0.105, 1.15×10⁻³)	N(50, 1.64×10⁻³)	N(300, 7.08×10⁻³)

Table 4 Partial random sampling data

| Sample	ΔR_L (mm)	ΔR_R (mm)	L_L (mm)	L_R (mm)
1	0.092	0.128	49.93	299.95
2	0.098	0.079	50.06	300.12
3	0.069	0.138	50.01	300.06
4	0.077	0.061	49.95	300.00
5	0.085	0.081	50.04	299.97
⋮	⋮	⋮	⋮	⋮
99	0.130	0.096	49.97	300.01
100	0.046	0.065	50.08	300.01

corresponding variance of each sample is shown in Fig. 15.

4 Comparison method of sensitivity indices based on PCE surrogate model

The purpose of sensitivity analysis is to guide tolerance allocation and satisfy kinematic and dynamic
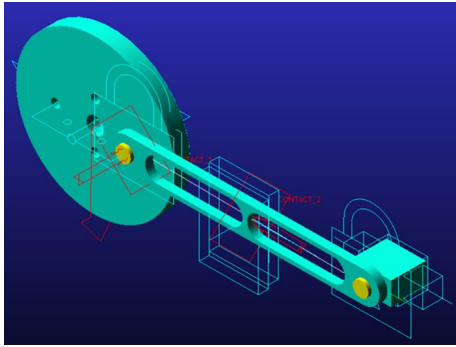
Fig. 14 Hybrid simulation model of the crank-slider mechanism
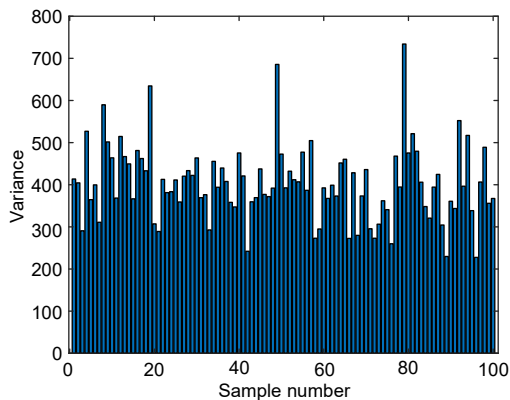
Fig. 15 Variance data of slider acceleration based on the hybrid simulation model

performances. Therefore, we defined the basis for evaluating the sensitivity indices by whether the tolerance scheme guided by each sensitivity could better meet the performance requirements. We also proposed a comparison method of sensitivity indices for kinematic and dynamic performances. Firstly, the sensitivity indices were calculated based on the PCE surrogate model, which was built based on the experimental data of the hybrid simulation model. Secondly, using the constraint function of cost-tolerance, the tolerance allocation scheme corresponding to each sensitivity index was solved according to the sensitivity results. Finally, each tolerance scheme was imported into the hybrid simulation model and the corresponding kinematic and dynamic performances were compared to determine the best sensitivity index for the transmission mechanism.

4.1 Surrogate model based on the PCE method

The PCE method is a very effective analysis method based on random uncertainty. It arises from the

theory of the Wiener homogeneous function (Wiener, 1938; Wiener and Teichmann, 1959).

The PCE method can be roughly divided into two steps:

(1) Construction of the PCE model. The input and output random variables are expressed as weighted linear combinations of a set of orthogonal polynomial basis functions.

(2) Calculation of the PCE coefficient. The weights of each orthogonal polynomial basis function are calculated.

We used the non-interference polynomial chaos expansion (NIPCE) method (Acharjee and Zabaras, 2007) of the PCE method to establish the surrogate model, which is widely used in engineering problems. For NIPCE, the PCE coefficient can be obtained by the stochastic response surface method (SRSM) (Isukapalli, 1999; Isukapalli et al., 2000).

The PCE surrogate model was built based on the experimental data of the hybrid simulation model. The specific process is as follows:

(1) The PCE model was constructed according to the mathematical model. Appropriate orthogonal polynomial basis functions were selected and combined according to the rules. The specific form depended on the set order.

(2) The PCE coefficient was calculated by the SRSM. We input 100 groups of sample data, including input variable values and output variance values. Part of the sample data was used for the PCE coefficient calculation, and the number of groups required also depended on the set order, while the other part of the sample data was used for model testing.

(3) The obtained PCE surrogate model was used to calculate the output variance corresponding to the original 100 groups of input variables, and the percentage error and standard error (RMSE) between the original variance and the output variance were calculated. The different-order PCE surrogate models were evaluated, and the third-order one was the optimal order. The percentage error in the third order is shown in Fig. 16.

Furthermore, the RMSE of the third-order PCE is 1.132. It was proved that this model could effectively restore the numerical relationship between output variance and input variables in the hybrid simulation model.
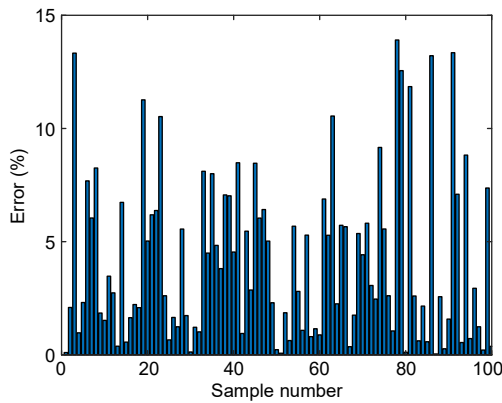
Fig. 16 Approximation error of the PCE surrogate model

4.2 Sensitivity calculation based on the PCE model

For the above four sensitivity indices, the PCE surrogate model is used to obtain the output response corresponding to specific input variables, so as to calculate their sensitivity. The specific process is as follows:

(1) Linear regression method

The PCE surrogate model is used to expand the sample size, and linear regression calculation is performed directly to obtain the expression as follows:

$$y = 14161 + 1296.6x_1 - 680.3x_2 + 107.1x_3 - 63.9x_4,$$

where y is the difference variance, x_1 is the value of ΔR_L, x_2 is the value of ΔR_R, x_3 is the value of L_L, x_4 is the value of L_R, and their units are all mm.

In this expression, the coefficients of x_2 and x_4 are negative, which is inconsistent with the actual situation of the model. Using multiple groups of sample sizes to re-calculate the linear regression, the obtained expression resembles the above. This model is not linear, and its higher-order effects are large enough that linear regression cannot be used to calculate the sensitivity of its output response to its input variables.

(2) Sobol method

The Sobol method is used to calculate the first-order sensitivity of the variance of the slider acceleration difference, which reflects the kinematic and dynamic performances of the mechanism, to each input variable (Saltelli et al., 2008). The calculation method is as follows: set two input sample matrices A and B with the same size N; take B as the original matrix and replace the ith column with the ith column of A to get matrix C; the corresponding output response

column vectors y_A, y_B, and y_{C_i} of each input sample matrix are obtained. The first-order sensitivity index can be calculated by

$$S_i^{(1)} = \frac{\frac{1}{N}\sum_{j=1}^{N} y_A^{(j)} y_{C_i}^{(j)} - f_0^2}{\frac{1}{N}\sum_{j=1}^{N} \left(y_A^{(j)}\right)^2 - f_0^2}, \tag{19}$$

where

$$f_0^2 = \frac{1}{N}\sum_{j=1}^{N} y_A^{(j)}. \tag{20}$$

The convergence value is shown in Fig. 17 as the sample size changes.
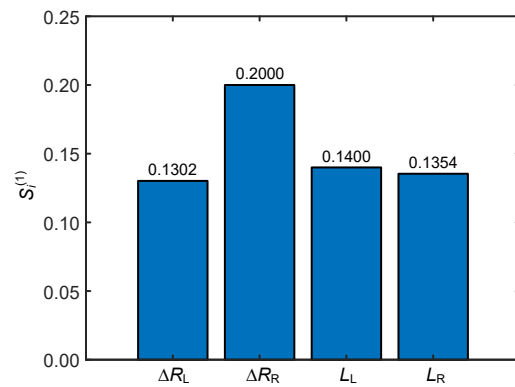

Fig. 17 First-order Sobol sensitivity indices

(3) Moment-independence method

The PCE surrogate model is used to calculate the output response corresponding to a specific input sample. Eqs. (13)–(15) are used to calculate the moment-independent sensitivity index $S_i^{(PDF)}$ based on the PDF. The convergence value is obtained by changing the sample size, as shown in Fig. 18.

(4) Information-entropy method

The method of information-entropy is like the method of moment-independence. Eqs. (16)–(18) are used to calculate the global sensitivity index S_{x_i} of information-entropy. The convergence value is obtained by changing the sample size, as shown in Fig. 19.

4.3 Tolerance allocation based on the sensitivity

In this study, sensitivity and cost-tolerance functions are combined to allocate tolerance. Given a total cost value, the cost was allocated according to the
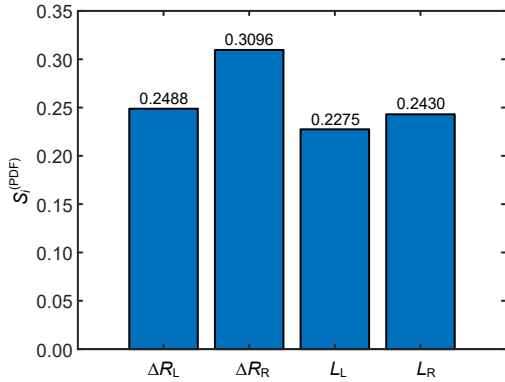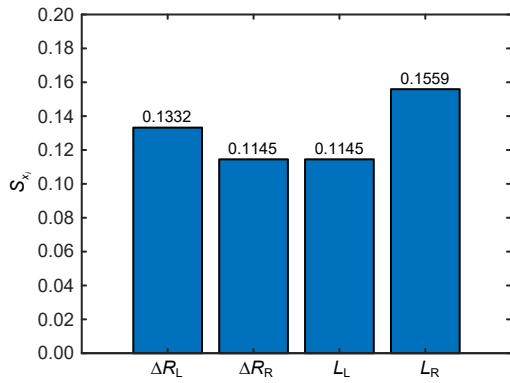
Fig. 18 Moment-independent sensitivity indices

Fig. 19 Information-entropy sensitivity indices

proportional relationship between the sensitivity indices of the input variables. Then, the tolerance range of each mechanism part size corresponding to the input variable was calculated by combining the cost-tolerance functions. The tolerance allocation scheme corresponding to each sensitivity index was obtained.

The cost-tolerance function (Mo et al., 2011) used is as follows:

(1) Machine cost-tolerance model of the outer circle feature size:

$$C(T) = 15.1138e^{-42.2874T} + \frac{T}{0.8611T + 0.01508}, \quad (21)$$

where T is the dimensional tolerance, and its unit is mm.

(2) Machine cost-tolerance model for locating feature size:

$$C(T) = \begin{cases} 8.2369e^{-35.8049T} + 1.3071^{\frac{-0.0083}{T}}, & T \leqslant 0.13, \\ 1.23036, & T > 0.13. \end{cases} \quad (22)$$

We assume that the total cost is 5, and the reasons are as follows: the input samples of the hybrid simulation model are sampled based on the tolerance grade of IT12, so the tolerance allocation should be within this tolerance grade, and the fit limit clearance of connecting shaft in tolerance grade of IT12 is 0.42 mm; the tolerance allocation is determined by the cost allocation, which is based on the sensitivity index, and the sensitivity index of each mechanism part is not very different. The tolerance cost and tolerance range of each mechanism part size of the mechanism corresponding to the input variables are shown in Table 5.

4.4 Comparison of sensitivity indices based on kinematic and dynamic performances

Based on obtaining the tolerance scheme of each sensitivity index, it was assumed that the size of parts obeys normal distribution within the tolerance range. The LHS method was used to sample each part size, and the sample size of each tolerance scheme was 40 groups. The sample data were input into the hybrid simulation model in turn, and the slider acceleration data of two cycles at 300 r/min were obtained. Summary data of slider acceleration corresponding to each sensitivity index are shown in Figs. 20–22.

After subtracting each acceleration term from the acceleration degree of the slider of the ideal non-clearance mechanism at the same speed, the variance of the difference value is obtained. Each sensitivity index has 40 variances, the average of which is shown in Table 6.

**Table 5 Tolerance cost and tolerance range of each mechanism part size**

Variable	Tolerance cost			Tolerance range (mm)		
	Sobol method	Moment-independence method	Information-entropy method	Sobol method	Moment-independence method	Information-entropy method
S_L	1.0751	1.2090	1.2855	0.2100	0.1000	0.0919
S_R	1.6515	1.5043	1.1051	0.0721	0.0781	0.3505
L_L	1.1557	1.1057	1.1048	0.1075	0.1173	0.1175
L_R	1.1177	1.1810	1.5045	0.1146	0.1036	0.0765
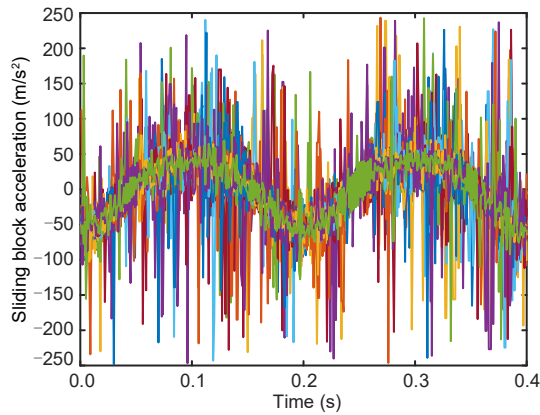
Fig. 20 Slider acceleration data based on the Sobol index
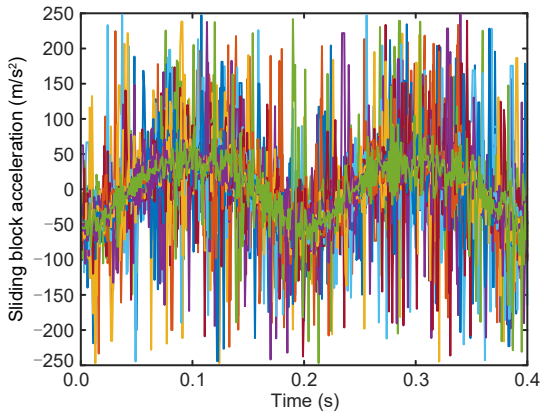
Fig. 21 Slider acceleration data based on the moment-independence index
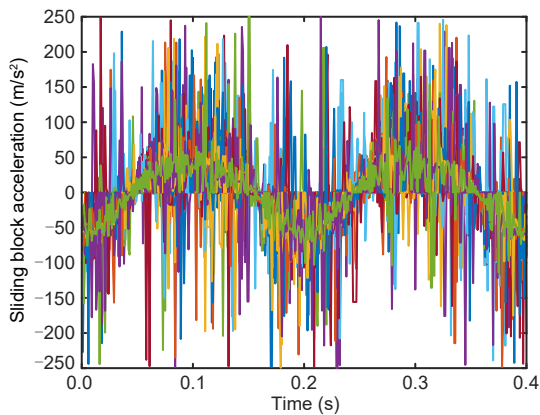
Fig. 22 Slider acceleration data based on the information-entropy index

Table 6 Sensitivity indices corresponding to the mean-variance

Index	Mean-variance
Sobol index	807.90
Moment-independence index	1112.12
Information-entropy index	1369.98

The curve in Fig. 20 is more concentrated near the ideal curve than those in Figs. 21 and 22. Among all the mean-variance of sensitivity indices, the mean-variance of the Sobol index is the smallest. Therefore, it can be considered that the Sobol index is the most appropriate sensitivity index for the transmission mechanism. When the researcher allocates tolerances to the transmission mechanism, the Sobol sensitivity analysis method can be used to assist the tolerance design, which can help the researcher determine the main effect of each input variable on the output response and optimize the kinematic and dynamic performances of the transmission mechanism.

5 Discussion

Compared with the other sensitivity analysis methods in this study, the Sobol sensitivity analysis method can better optimize the kinematic and dynamic performances of the crank-slider mechanism for tolerance allocation because the first-order Sobol index can effectively extract the main effect of each input variable in the nonlinear model on the response, but not the total effect. This is very important for sensitivity analysis of complex models such as transmission mechanisms because the total effect of each input variable on the response includes redundancy. The more complex the model is, the more attention should be paid to the redundancy, which will enlarge the effects of some input variables on the model response.

By comparing Figs. 17–19, it can be found that in the first-order Sobol index, the joint clearance ΔR_{R} has the largest proportion of sensitivity, while in the information-entropy index, ΔR_{R} has the smallest proportion of sensitivity. Therefore, the first-order Sobol index is more reasonable, because the slider is jointed with the right end of the connecting rod, where ΔR_{R} has the greatest effect on the kinematic and dynamic characteristics of the slider. What makes Fig. 19 so unusual is that it over calculates the total effects of some input variables on the model response.

Although this study is based on the comparative study of sensitivity analysis methods of typical transmission mechanisms, the best sensitivity analysis method obtained by comparison is not suitable for all transmission mechanisms. This is because the kinematic and dynamic performances of the transmission mechanism

are affected by the transmission type, and the Sobol method has requirements for independent inputs, which not all transmission mechanisms can meet. However, when the transmission form studied by the researcher resembles the crank-slider mechanism, this research is of value. At the same time, this study also points out the necessity for researchers to consider the total effect redundancy when performing sensitivity analysis on complex mechanisms.

In future research, we will propose a new sensitivity index, which will be suitable for more types of transmission mechanism and can be used in the presence of correlations among the inputs.

6 Conclusions

The kinematic and dynamic performances of the transmission mechanism are significantly affected by the geometric errors of the parts, and the tolerance design can make a reasonable geometric errors allocation of the parts while controlling the production cost. In this study, the crank-slider mechanism was used as the research object. Based on the proposed hybrid simulation model, the optimal sensitivity index for the transmission mechanism was determined by comparing multiple sensitivity indices and helped to achieve better tolerance design by assisting tolerance allocation.

(1) A hybrid simulation model was established based on the experimental data of the crank-slider experiment platform. The accuracy and reliability of simulation data are ensured when the experiment cost is reduced and the input variables are freely controlled.

(2) Based on the experimental data of the hybrid simulation model, a surrogate model based on the PCE method was established for the sensitivity calculation. It simplifies the calculation significantly.

(3) The tolerance was allocated based on the sensitivity and cost-tolerance function, and the tolerance scheme corresponding to each sensitivity index was obtained. Based on the kinematic and dynamic performances of the mechanism of each tolerance scheme, a new sensitivity evaluation method with engineering value is proposed.

Author contributions

Zhen-yu LIU designed the research. Han-chao XU and Guo-dong SA processed the experimental and simulation data. Guo-dong SA was in charge of the whole project. Yu-feng LYU assisted with the sampling and laboratory analyses. Jian-rong TAN gave theoretical guidance on the whole work.

Conflict of interest

Zhen-yu LIU, Han-chao XU, Guo-dong SA, Yu-feng LYU, and Jian-rong TAN declare that they have no conflict of interest.

References

Abbiati G, Marelli S, Tsokanas N, et al., 2021. A global sensitivity analysis framework for hybrid simulation. *Mechanical Systems and Signal Processing*, 146:106997.
https://doi.org/10.1016/j.ymssp.2020.106997

Acharjee S, Zabaras N, 2007. A non-intrusive stochastic Galerkin approach for modeling uncertainty propagation in deformation processes. *Computers & Structures*, 85(5-6):244-254.
https://doi.org/10.1016/j.compstruc.2006.10.004

Ambaye GA, Lemu HG, 2021. Dynamic analysis of spur gear with backlash using ADAMS. *Materials Today: Proceedings*, 38:2959-2967.
https://doi.org/10.1016/j.matpr.2020.09.309

Borgonovo E, 2007. A new uncertainty importance measure. *Reliability Engineering & System Safety*, 92(6):771-784.
https://doi.org/10.1016/j.ress.2006.04.015

Borgonovo E, Castaings W, Tarantola S, 2012. Model emulation and moment-independent sensitivity analysis: an application to environmental modelling. *Environmental Modelling & Software*, 34:105-115.
https://doi.org/10.1016/j.envsoft.2011.06.006

Cai M, Yang JX, Wu ZT, 2004. Mathematical model of cylindrical form tolerance. *Journal of Zhejiang University-SCIENCE*, 5(7):890-895.
https://doi.org/10.1631/jzus.2004.0890

Cao YL, Liu YS, Mao J, et al., 2006. 3DTS: a 3D tolerancing system based on mathematical definition. *Journal of Zhejiang University-SCIENCE A*, 7(11):1810-1818.
https://doi.org/10.1631/jzus.2006.A1810

Cao YL, Mathieu L, Jiang J, 2015. Key research on computer aided tolerancing. *Journal of Zhejiang University-SCIENCE A (Applied Physics & Engineering)*, 16(5):335-340.
https://doi.org/10.1631/jzus.A1500093

Cukier RI, Fortuin CM, Shuler KE, et al., 1973. Study of the sensitivity of coupled reaction systems to uncertainties in rate coefficients. I Theory. *Journal of Chemical Physics*, 59(8):3873-3878.
https://doi.org/10.1063/1.1680571

Dantan JY, Bruyere J, Vincent JP, et al., 2008. Vectorial tolerance allocation of bevel gear by discrete optimization. *Mechanism and Machine Theory*, 43(11):1478-1494. https://doi.org/10.1016/j.mechmachtheory.2007.11.002

Darlington RB, Hayes AF, 2016. Regression Analysis and Linear Models: Concepts, Applications, and Implementation. The Guilford Press, New York, USA, p.8-30.

Dubowsky S, Deck JF, Costello H, 1987. The dynamic modeling of flexible spatial machine systems with clearance connections. *Journal of Mechanisms, Transmissions, and Automation in Design*, 109(1):87-94. https://doi.org/10.1115/1.3258790

Haines RS, 1980. A theory of contact loss at resolute joints with clearance. *Journal of Mechanical Engineering Science*, 22(3):129-136. https://doi.org/10.1243/jmes_jour_1980_022_027_02

Helton JC, Davis FJ, 2003. Latin hypercube sampling and the propagation of uncertainty in analyses of complex systems. *Reliability Engineering & System Safety*, 81(1):23-69. https://doi.org/10.1016/S0951-8320(03)00058-9

Isukapalli SS, 1999. Uncertainty Analysis of Transport-Transformation Models. PhD Thesis, The State University of New Jersey, Piscataway, USA.

Isukapalli SS, Roy A, Georgopoulos PG, 2000. Efficient sensitivity/uncertainty analysis using the combined stochastic response surface method and automated differentiation: application to environmental and biological systems. *Risk Analysis*, 20(5):591-602. https://doi.org/10.1111/0272-4332.205054

Lin KS, Chan KY, Lee JJ, 2018. Kinematic error analysis and tolerance allocation of cycloidal gear reducers. *Mechanism and Machine Theory*, 124:73-91. https://doi.org/10.1016/j.mechmachtheory.2017.12.028

Liu YY, Guo JK, Li BT, et al., 2019. Sensitivity analysis and tolerance design for precision machine tool. *Journal of Mechanical Engineering*, 55(17):145-152 (in Chinese). https://doi.org/10.3901/JME.2019.17.145

McKay MD, Beckman RJ, Conover WJ, 2000. A comparison of three methods for selecting values of input variables in the analysis of output from a computer code. *Technometrics*, 42(1):55-61. https://doi.org/10.2307/1271432

Mo S, Li ZL, Li Y, et al., 2011. Concurrent tolerance optimization design based on time value of money. *Journal of Machine Design*, 28(11):85-89 (in Chinese). https://doi.org/10.13841/j.cnki.jxsj.2011.11.019

Saltelli A, Tarantola S, 2002. On the relative importance of input factors in mathematical models: safety assessment for nuclear waste disposal. *Journal of the American Statistical Association*, 97(459):702-709.

https://doi.org/10.1198/016214502388618447

Saltelli A, Ratto M, Andres T, et al., 2008. Global Sensitivity Analysis: the Primer. John Wiley & Sons Ltd., West Sussex, UK, p.1-165.

Seneviratne LD, Earles SWE, Fenner DN, 1996. Analysis of a four-bar mechanism with a radially compliant clearance joint. *Proceedings of the Institution of Mechanical Engineers, Part C: Journal of Mechanical Engineering Science*, 210(3):215-223. https://doi.org/10.1243/PIME_PROC_1996_210_191_02

Shannon CE, 1948. A mathematical theory of communication. *The Bell System Technical Journal*, 27(3):379-423. https://doi.org/10.1002/j.1538-7305.1948.tb01338.x

Sobol IM, 1993. Sensitivity estimates for nonlinear mathematical models. *Mathematical Modelling and Computational Experiments*, 1:407-414.

Sobol IM, 2001. Global sensitivity indices for nonlinear mathematical models and their Monte Carlo estimates. *Mathematics and Computers in Simulation*, 55(1-3):271-280. https://doi.org/10.1016/S0378-4754(00)00270-6

Soong K, Thompson BS, 1990. A theoretical and experimental investigation of the dynamic response of a slider-crank mechanism with radial clearance in the gudgeon-pin joint. *Journal of Mechanical Design*, 112(2):183-189. https://doi.org/10.1115/1.2912591

Sudret B, 2008. Global sensitivity analysis using polynomial chaos expansions. *Reliability Engineering & System Safety*, 93(7):964-979. https://doi.org/10.1016/j.ress.2007.04.002

Tian Q, Flores P, Lankarani HM, 2018. A comprehensive survey of the analytical, numerical and experimental methodologies for dynamics of multibody mechanical systems with clearance or imperfect joints. *Mechanism and Machine Theory*, 122:1-57. https://doi.org/10.1016/j.mechmachtheory.2017.12.002

Wiener N, 1938. The homogeneous chaos. *American Journal of Mathematics*, 60(4):897-936. https://doi.org/10.2307/2371268

Wiener N, Teichmann T, 1959. Nonlinear problems in random theory. *American Institute of Physics*, 12(8):52. https://doi.org/10.1063/1.3060939

Zhou SE, 2019. Assembly Modeling and Accuracy Analysis Method of Complex Product Based on Digital Twin. PhD Thesis, Zhejiang University, Hangzhou, China (in Chinese).

Ziegler P, Wartzack S, 2015. A statistical method to identify main contributing tolerances in assemblability studies based on convex hull techniques. *Journal of Zhejiang University-SCIENCE A (Applied Physics & Engineering)*, 16(5):361-370. https://doi.org/10.1631/jzus.A1400237